Phototunable Mechanical Properties of Azobenzene-Containing Hydrogels

By

Bradly Bennet Baer

Thesis
Submitted to the Faculty of the
Graduate School of Vanderbilt University
in partial fulfillment of the requirements
for the degree of

MASTER OF SCIENCE
in

Interdisciplinary Materials Science
August, 2016
Nashville, Tennessee

Approved:

Leon M. Bellan, Ph.D.

D. Greg Walker Ph.D.

ACKNOWLEDGEMENTS

I would like to thank the other members of my lab, without whom this work would not have been finished, for their advice and support. Special thanks to Brian O'Grady for his help with the acquisition of the rheological data, as well as his assistance with the testing of the cytocompatibility of the ADA-Gelatin hydrogels. I would also like to thank Alice Leach for graciously offering to proofread significant portions of this document.

TABLE OF CONTENTS

Page

LIST OF TABLES

LIST OF FIGURES

CHAPTER 1

INTRODUCTION

Since its beginnings in the 1980's, the multidisciplinary field of tissue engineering has grown as increased effort is focused on developing biological substitutes to restore, replace, or regenerate defective tissues. Tissue engineering has three main components: a scaffold, cells, and growth factors. These elements are sometimes referred to as the triad of tissue engineering.[1]

Scaffolds are typically made from biocompatible polymers, especially polymers that can swell in water to form a hydrogel, because hydrogels inherently mimic the conditions of the human body, which is roughly 60% water itself. They are also commonly three dimensional, similar to most tissues in the body, as cells are known to behave differently when grown in monolayer culture versus three dimensional culture.[2] There are a large variety of hydrogels that may potentially be used as scaffolds, and in order to understand the slight differences between them it is important to understand the role that scaffolds play in an artificial tissue construct.[1] The purpose of the scaffold is to replicate the function of the extra-cellular matrix (ECM), which is the network of proteins that defines the volume of biological tissues, fills the space between cells, and provides support and attachment points for cells.[3] That is to say, the scaffold performs three primary functions: architectural, biological, and mechanical.

The architectural function of the ECM is complex and can be difficult to replicate completely with an artificial scaffold. For example, the collagen fibers in tendons are well-organized and highly resistant to stretching, giving tendons their high tensile strength. On the other hand, randomly distributed collagen and elastin in skin tissue is responsible for the tissue's

characteristic toughness and elasticity.[1] It is possible to take a tissue sample and remove the cells to leave behind a decellularized matrix, but for true scalability the scaffold must be created de novo due to the time and cost associated with the decellularization of a natural matrix.[4,5] The scaffold must be able to fully define the engineered tissue volume, but also have enough porosity to accomplish a few specific functions. If the scaffold is to be seeded with cells throughout its volume, there must be enough void volume for cells to be distributed through the scaffold or the cells must be able to degrade the constituent material in order to create their own pathways for propagation. Similarly, porosity or cellular degradability to encourage ingrowth of both host tissue and vascularization is important, such that the artificial tissue can be fully integrated with its host. Additionally, the scaffold must be porous enough to allow for nutrient diffusion during the pre-implantation phase where it is initially seeded with cells and before vascularization has been established in the scaffold. Finally, the scaffold must be made of a material that is biodegradable, as the goal of tissue engineering is not to replace natural tissues, but to guide the body's natural healing processes in the restoration of natural tissue.[6] Ideally the rate of degradation should be roughly equal to the rate of host integration, such that the scaffold will deteriorate as the host tissue integrates the construct into itself. Therefore the repaired tissue is virtually indistinguishable from natural tissue.

The next function of the scaffold is biological. It should mimic the natural behavior of the ECM that a cell would normally be found in. This is a requirement for virtually any cell, since the only cells that routinely exist unsupported are blood cells. It is not enough that the matrix simply exist and the cells be placed within it; the matrix must be attractive to the cells in some way that the cells are able to sense. Natural ECM components may have bioactive regions that provide cells with cues on regulating their activities. For example, fibronectin is a common ECM

protein that has the peptide sequence RGD, which offers binding sites for cells that come in contact with it, leading to enhanced cell adhesion. In contrast, synthetic polymers such as polyethylene glycol (PEG) can be used to form hydrogel scaffolds and are biocompatible, but have no "features" visible to cells, and thus have poor cell adhesion and must be functionalized to increase cell adhesion. Additionally, the repeating structural patterns of fibronectin can encourage the natural directional alignment of the cells attached to the matrix.[7,8]

The final function of the scaffold is mechanical. At the most basic level, the scaffold must be able to support its own weight, as well as be mechanically robust enough to survive handling/implantation and the ensuing healing/ingrowth process. Additionally, the scaffold must be appropriately matched to the cells within it, as well as the tissue that it is attempting to mimic. Cells are able to sense the mechanical properties of their surroundings, generally represented by the modulus of the material, suggesting that the stiffness of the scaffold is important in addition to the biological functionality of the scaffold.[9] For example, hard tissue cells such as bone cells will not proliferate as well on a scaffold with the same modulus as adipose tissue as they would on a stiffer scaffold, even in the presence of binding sites.[10]

Once a scaffold mimicking the appropriate properties of the target tissue has been selected, the next building block of the tissue engineering process is the cells that will grow on it. Despite a myriad of choices for the scaffold, there are typically only two sources for the cells. The first possible category is primary cells obtained by harvesting healthy cells from the patient; these can then be grown into the scaffold and used to repair damaged tissue.[11,12] This method works for wound healing, but can have difficulty repairing diseased tissue if no suitable healthy cells can be located, or if the harvesting of healthy cells poses a risk to the patient. In these situations, the solution is to use stem cells.[13] Advances in medical technology have enabled the

possibility of using induced pluripotent stem cells (IPSCs), which are healthy patient primary cells that have been regressed into stem cells. These can then be differentiated into the cell type needed for treatment.

The final element of tissue engineering is growth factors. These are a class of small molecules and proteins that interact with cells in order to stimulate growth, proliferation, healing, and differentiation. Growth factor choices are limited, as each growth factor accomplishes a specific function and is non-interchangeable.[14,15] There are known and proven combinations of media, growth factors, and inhibitors that are used to keep specific types of cells alive in culture, as well as differentiate stem cells into specific primary cell lines if stem cells are used. Some of the reagents required are quite expensive and pose a challenge when attempting to culture multiple cell types in close spatial proximity due to different growth factor requirements for each cell type. Any developments that reduce the need for growth factors have the potential to increase the scalability and reduce the cost of tissue engineering.

Since the field of tissue engineering is a combination of engineering and biology, and the primary contribution of the engineering side is the design of the scaffold, much research has been done in designing different scaffold types. There are a variety of different hydrogel formulations for use as scaffolds, with a variety of backbone structures, crosslinking methods, and viability enhancing side groups. Polymers sponges and foams are also used, which do not swell in water but maintain structural stability with very high porosities of above ~90%. They are generally made using particle leaching techniques to leave behind an highly porous structure with empty pores.[16-18] The majority of these scaffolds are static in their properties; they are formulated with a specific set of properties and those properties remain constant or degrade as the scaffold itself degrades. This leaves a significant gap in knowledge for the field of tissue engineering. Tissues

in the body rarely experience static conditions. The ECM in natural tissues is constantly being degraded, rebuilt, and modified by the cells that reside in the tissue.[19] This is in stark contrast to the static scaffolds that are used. It would therefore be beneficial to the field to have tissues that can be dynamically tuned so that the way cells respond to environments that have changing mechanical properties can be studied in a controlled setting.

There have been several literature reports of scaffolds that have tunable mechanical properties, but all possess some drawbacks. The first method that was used to create gels with tunable properties involved reversible crosslinker units. Lin *et al.* developed a polyacrylamide hydrogel in which they replaced the traditional chemical crosslinking units with complimentary strands of DNA.[20] Two methods were used to reverse these crosslinkers. In the first, samples were heated. The amount of thermal energy required to break the hydrogen bonding between the two DNA strands was calculated and then applied to the gel to tune its mechanical properties. In the second, toehold segments on the crosslinkers were used so that unbound strands of DNA could be added to the gel to compete with crosslinker segments and reduce crosslinker density. In a follow-up paper, Jaing *et al*. showed that the presence of exogenous DNA had no effect on the growth of two types of fibroblast, but that they did respond to changes in the mechanical properties of the gel caused by changes in the crosslinker. The response of the fibroblasts was also dependent on the magnitude of the change in mechanical properties.[21] In a similar manner, Gillette et al. developed a two-component hydrogel in which one component, collagen, was designed to provide structural support and cell adhesion sites, and the second component, alginate, had tunable crosslinking based on its ability to bind with a divalent cation such as Ca^{2+}. The crosslinking action of Ca^{2+} was undone through the use of a chelating compound that binds to 2+ ions, which was delivered in the biocompatible form of sodium citrate.[22]

A pH responsive hydrogel was developed by Yoshikawa *et al.* using a pH responsive triblock copolymer. The synthesized a biocompatible ABA triblock polymer that contained a pH responsive block that changed conformation in response to pH changes. Using a pH of between 7 and 8 they were able to reversibly modify the modulus of the hydrogel buy up to a factor of 40.[23] This methodology may work in culture, but under the physiological conditions than an implant would experience it would become very difficult to control the pH of the hydrogel or prevent it from equilibrating to the host's physiological pH.

A different mechanism for tuning the mechanical properties of a hydrogel was developed by Kong et al. in the form of an engineered protein that was able to fold and unfold in response to changes in the oxidation state of a disulfide bond. This leads to a dramatic change in the protein's effective length as well as the mechanical properties of the protein itself.[24] The protein was designed such that it could be integrated into a hydrogel as a crosslinking unit through a well-developed photocrosslinking method.[25] The reduced and oxidized states were achieved through the use of dithiolthreitol (DTT) and hydrogen peroxide. The effects of these chemicals and the changes in oxidation state that they cause were not tested on cells; only the mechanical properties of the gel were investigated.

Systems that can be manipulated with light offer an alternative control route to chemical control; one that does not require the addition of reagents from an outside source. Kloxin *et al*. developed PEG scaffolds with a photodegradable unit located adjacent to the crosslinking site.[26] With harmless levels of UV light, the modulus of the gel can be reduced significantly by reducing the crosslinking density through photolysis. Similarly, Guvendrien *et al*. used a hyaluronic acid based system that was able to undergo sequential addition and radical polymerization crosslinking reactions in response to UV light.[27] This led to an increase in the

modulus of the gel in response to light exposure. Both systems allow for spatial and temporal control over the changes in modulus, but both can only go in one direction, stiffer or softer, and are irreversible.

All of these methods possess the ability to manipulate the mechanical properties of the scaffold, but they also come up short in important ways. Some require the addition of external reagents that may interact indiscriminately with cells embedded in the scaffold rather than their intended targets, and others provide mechanical tunability in an irreversible manner.

One of the more promising platforms for the reversible and non-invasive control of the properties of a hydrogel matrix is the use of a photoisomer, principally azobenzene compounds. Azobenzene compounds have been used to control other properties in hydrogels such as the gel-sol transition and the swelling ratio.[28-31] The photoisomerization of azobenzenes was first reported in 1937 and has been used in a variety of other fields.[32-36] This has led to the development of a large body of knowledge on the function of azobenzenes. They are of particular interest in biology because they absorb light in a biologically compatible region (350-550nm).[37] In small molecule systems, azobenzene photoisomerizes from the trans to cis isomer in a very efficient reaction (80-95% conversion). Removal of the UV light or irradiation with visible light can regenerate the trans isomer with yields >99% due to the large thermodynamic driving force.[38]

Azobenzene has found a very specific niche in biology due to its regulating ability through changes in effective molecular length. Due to its photoisomerization, azobenzene containing caps can be put on the ends of ion channels allowing neurons to be fired remotely using UV light.[39] This method has also been adapted to drug delivery; the pores in mesoporous

Si nanoparticles are capped with photoresponsive azobenzen derivatives and targeted drug delivery is achieved through the selective irradiation of diseased tissues with UV light.[40]

Azobenzene compounds do not require an initiator of any kind; the photoismoerization reaction proceeds with light alone. There are no reactive species produced, and no free radicals. Additionally, the light stimulus can be introduced noninvasively and requires no modification of the chemical environment of the scaffold. Moreover, the azobenzene molecule undergoes structural changes related to rotation about a bond only, so we expect that photoisomerization can occur without changing the connective properties of the matrix.

In the work presented here, an azobenzene derivative, azodianiline (ADA), is incorporated into a gelatin based hydrogel using microbial transglutaminase (mTG) in order to modulate the mechanical properties of the resulting hydrogel using 365 nm light and broad spectrum white light. The photoisomerization has been reported to disrupt the hydrogen bonding in loosely associated portions of the hydrogel, leading to a reduction in mechanical properties that can be fully reversed upon heating or exposure to visible light.[38]

CHAPTER 2

METHODS

2.1 Light Sources

The same light source was used for all experiments. Two LEDs were attached to the same heatsink using thermal adhesive. One LED was a 2.9W UV LED (365nm, LED Engin LZ4-44UV00-0000) and the other was a white light LED. Both LEDs were run using the same power supply, with the white LED being run with 0.6A at 3.2V and the UV LED being run with 0.6A at 15V.

2.2 Hydrogel Formation

Gelatin samples were synthesized according to the following recipes for the 5/10/15% gelatin hydrogels: 5/10/15 g gelatin powder (Porcine, Sigma Aldrich) was added to 100 mL of 1x Phosphate Buffered Saline(PBS) (Fisher Scientific) and was dissolved while boiling under reflux. The solution was boiled for 1 hour and then sterile filtered with a 0.22 μm filter (Millipore) under sterile conditions. The crosslinker, food-grade microbial transglutaminase (mTG) (Modernist Pantry) was dissolved in 1x PBS at a concentration of 0.1 g/mL and sterile filtered. Crosslinked gels were made by mixing the appropriate gelatin solution with mTG in a 4:1 ratio. Mixed gels were poured into molds and left in an incubator overnight to crosslink completely. After 30 minutes of crosslinking, 1x PBS was poured over the mold to completely submerge the gels and allow them to swell to equilibrium as they cured.

Azodianiline (ADA) (Sigma Aldrich) containing gels were synthesized as follows. A stock solution of ADA was made with ADA dissolved in ethanol at a concentration of

0.1 g/50 mL. This stock solution was added to the gelatin solution to create gels with the appropriate ADA concentration. The standard amount of ADA added was 50 μL of stock solution per 10 mL of total hydrogel volume, to give a total ADA concentration of 0.001% by weight, which is denoted by N, or normal ADA. This value was decided based on a desire to minimize the amount of ethanol added to the system to preserve the system's utility for work with cells. Samples denoted with D had double the ADA amount, or 0.002% by weight. The volume contribution from the ADA solution was small and was neglected when calculating the gelatin percentages.

All hydrogel formation was carried out under sterile conditions to prevent the possibility of contamination altering the mechanical properties of the gels.

2.3 Instron Tests

Mechanical testing was carried out on an Instron 5544 load cell with a 2 kN load cell and compression platens installed. Samples for compressive testing were prepared in molds with a diameter of 13 mm and filled with a total volume of 2 mL to produce cylinders with nominal dimensions of 12 mm diameter by 14 mm height. Tests were conducted at a crosshead movement rate of 2 mm/min at room temperature. Load and extension were recorded and sample dimensions were used to convert load and extension into engineering stress and strain. Samples were run in triplicate and the moduli of the gels were taken from the 2-8% strain region.

ADA-Gelatin samples were irradiated with UV light in a light-box with a 365 nm 2.9 W luminous flux UV LED (LED Engin) from a distance of 6 inches for 5 minutes. The samples were then removed from the box, measured to account for any possible dimensional changes, and tested in a dark room to protect from incidental light exposure. Finally, the samples were irradiated with white light for 5 minutes to test the reversibility of the modulus change.

2.4 Rheology Measurements

Rheological measurements were collected with an AR2000 (TA Instruments). Disposable top and bottom plates were used and the gel was adhered to the top and bottom plates with superglue (Loctite 4541) during testing to prevent dimensional changes during irradiation from breaking contact with the plates. A heated stage was used to ensure that the sample remained at 37°C for the duration of the test. The UV and White LEDs were placed 6 inches away from the sample and the entire apparatus was shrouded with a blackout curtain to protect it from light exposure. Samples were run once and discarded to prevent any effects repeated stress cycling.

Data was analyzed and exported using TA's Universal Analysis software suite.

2.5 Confocal Microscopy

Gels were made from the same stock solutions. The 10% gelatin was chosen for the confocal experiments. A stock solution of fluorescent polystyrene beads was made by diluting a purchased solution of 2 μm polystyrene beads (Invitrogen) 1:100 in PBS. This stock solution was sonicated to break up agglomerates then filtered through a 5 μm filter to remove any remaining agglomerates. The filtered solution was then autoclaved to ensure sterility as the beads were an order of magnitude too large to allow sterile filtering (0.22 μm for sterile filter). A single drop of the bead solution was imaged using a fluorescent microscope after autoclaving to confirm that the sterilization did not damage the beads in solution or reduce their fluorescence. The gels were made as described above but 1 mL of the bead stock solution was added to the gel solution and thoroughly mixed to disperse the beads. The gels were poured in a petri dish and left in an incubator overnight with a layer of water over the top of the gel to allow the gel to swell to equilibrium and prevent drying.

The gels were imaged on a Zeiss 710 confocal microscope. Samples were tested for a total of 40 minutes, with 10 minutes per experimental condition. The 4 experimental conditions were in the following order: 1) 10 minutes of no light to get a background; 2) 10 minutes of UV light exposure; 3) 10 minutes of no light; 4) 10 minutes of white light exposure. Images were taken once every 6 seconds, to produce 10 images per minute and 100 images per experimental condition. Each condition was run immediately after the previous condition. Samples were discarded after one run to prevent error from repeated stress and relaxation events.

The image stacks were analyzed using the TrackMate plugin in FIJI.[41] The spot analysis was run with an estimated blob diameter of 5 μm and a threshold of 7.5. The algorithm was allowed to automatically discard particles that did not meet quality noise, and these discarded particles were assumed to be noise. The particle tracing algorithm was run using a maximum linking distance and gap-closing max distance of 5 μm, and with a maximum frame gap of 2 frames. The algorithm exported the particle trace identifiers, the number of frames each particle appeared in, and the total distance traveled by each particle.

CHAPTER 3

RESULTS & DISCUSSION

To obtain a hydrogel with tunable mechanical properties, we mixed small amounts of ADA (0.001% or 0.002% by weight) into gelatin solutions and crosslinked them with microbial transglutaminase (mTG), which is an enzyme that binds a free amine group, from the side chain of a lysine, to the acyl group at the end of a glutamine side chain. Both of these amino acids are present in gelatin. ADA has a free amine on either end (Figure 1). While this amine is more sterically hindered than that of a lysine side chain, the enzyme can still crosslink it into the gelatin network as it crosslinks the gelatin network itself. The ADA turned the gelatin hydrogel a bright shade of yellow, indicating that ADA was incorporated into the gel (Figure 2). However, the water bath that the gels swelled in turned yellow as well, indicating that a portion of the ADA did not get integrated into the gelatin network. The samples were irradiated with UV light and exhibited a dimensional change, including tearing when exposed to too much UV light, which was taken as evidence that at least a portion of the ADA was being crosslinked into the gelatin structure. We attempted an alternate crosslinking method using modified gelatin (GelMA) and a photoinitiated curing agent (Irgacure, BASF), but the ADA proved to be significantly more effective than the curing agent at absorbing the UV radiation. Therefore, in this case the hydrogel could not be crosslinked using a photocuring method.

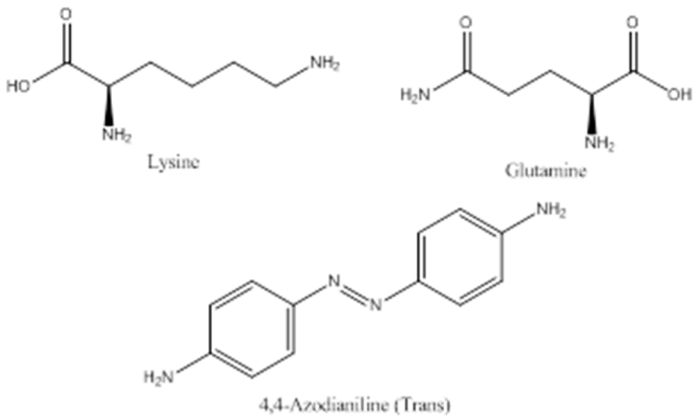

Figure 1. Structures of molecules involved in crosslinking. ADA is presented in its *trans* isomer.

Figure 2: Comparison of a control hydrogel (left) with a hydrogel containing 0.001% ADA (right).

We irradiated the ADA stock solution with white light when it was made and stored it in a brown glass bottle at room temperature to protect it from incidental UV exposure. All ADA in the stock solution should have been converted to and maintained in the *trans* state during storage and subsequent integration into a ADA-Gelatin network. As the *trans* isomer of ADA is also

more thermodynamically stable, time spent in the incubator would also strongly favor the *trans* isomer. Therefore, the ADA in the ADA-Gelatin hydrogels should be completely in the *trans* isomer at the beginning of each experiment.

Confocal microscopy was used to determine the amount of motion caused by the UV exposure on a microscopic level. Each field of view had a significant number of particles that were tracked. Representative fields of view are shown in Figure 3. The single images are flattened time series, representing 10 minutes of particle tracking. The particles were divided into two categories based on the percentage of total frames that the particle appeared in. This was to exclude particles that moved in and out of the focal plane during the duration of the experiment. The experimental conditions necessary to capture a field of view with a sufficiently large number of particles led to a ratio of 14:1 for XY:Z pixel dimensions. This ratio does introduce the risk that we are underestimating the amount of motion experienced by a particle, but the uncertainty added in including motion in the z-direction was deemed too great.

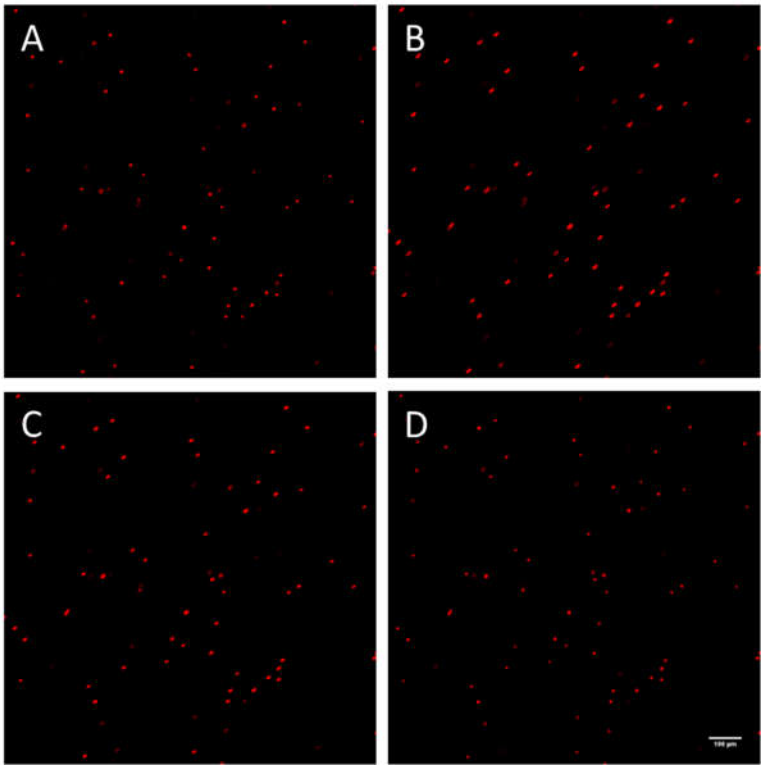

Figure 3. Flattened time series of fluorescent bead motion under specific light conditions. A) No light, before UV exposure B) UV exposure, C) No light, after UV exposure D) White light exposure. Motion in panels B and C are in opposite directions; all images share the same scale bar of 100 µm.

Table 1 contains the average particle motion in response to UV exposure. It must be noted that there was virtually no difference in the amount of motion detected between the no light condition and the white light condition. In theory, the white light should have caused the ADA to convert back to the *trans* isomer and undo the motion observed when the UV irradiation occurred. Interestingly, motion in the reverse direction occurred during the period between UV irradiation and white light irradiation. This can be explained by the experimental conditions. The fluorescent beads that were being used to track the contraction of the scaffold were red-emitting beads. Their excitation wavelength was green light, which was provided by an Argon laser at 514 nm. Therefore, in all conditions there is exposure to wavelengths of light that can cause the photoisomerization of ADA from *cis* back to *trans*. This indicates that the true amount of motion

possible is significantly greater than that which these experiments show, as a high intensity focused laser should be very effective in providing photons to an absorber as efficient as ADA

Light Condition	Number of particles	Avg. # Frames Present	Avg. Displacement (μm)	Number of particles in 50%+ frames	Avg. # Frames Present (50%+)	Avg. Displacement (50%+) (μm)
Pre-UV	227	32.16	1.34 ± 0.33	60	91.73	2.31 ± 0.30
UV	229	31.62	3.18 ± 0.33	50	87.98	8.33 ± 0.54
Post-UV	246	31.13	2.24 ± 0.31	64	87.59	5.23 ± 0.59
White	301	28.21	1.06 ± 0.17	70	88.22	1.26 ± 0.31
Control-UV Exposure	298	30.83	1.90 ± 0.19	68	76.34	3.19 ± 0.34

Table 1. Measurements of the motion of fluorescent beads in ADA-Gelatin under different light exposure conditions. Data was split into two sets; particles that were visible in more or less than half of the available frames. The first four rows represent motion in an ADA-Gelatin hydrogel. The final row is a control sample with no ADA.

The amounts of motion that were observed were not even. During the period of time immediately after the end of UV exposure, the fluorescent beads were seen moving approximately two thirds of the way back towards their original positions. This indicates that either 10 minutes was too long an exposure time and the gel experienced deformation that left the elastic region, or that there was a portion of the contraction that was non-local, which is to say contraction that occurred outside of the field of view that was being directly imaged. The non-local contraction could not have been reversed by the laser light. Thus when the white light was applied, this non-local relaxation was not distinguishable from background motion.

A control sample consisting of only gelatin with no ADA component was run under the same conditions and the motion of the fluorescent beads was recorded. The control sample exhibited some motion, but significantly less than that exhibited by ADA-Gelatin hydrogels under exposure to UV. A possible explanation for the motion of the beads in the control sample when exposed to UV is the addition of thermal energy and thermal expansion. The UV LED outputs a considerable amount of power, which may be converted to heat in the hydrogel. The microscope was equipped with a heated stage to maintain physiological temperatures, but it is designed to maintain a constant elevated temperature and is not equipped to counteract additional heat sources.

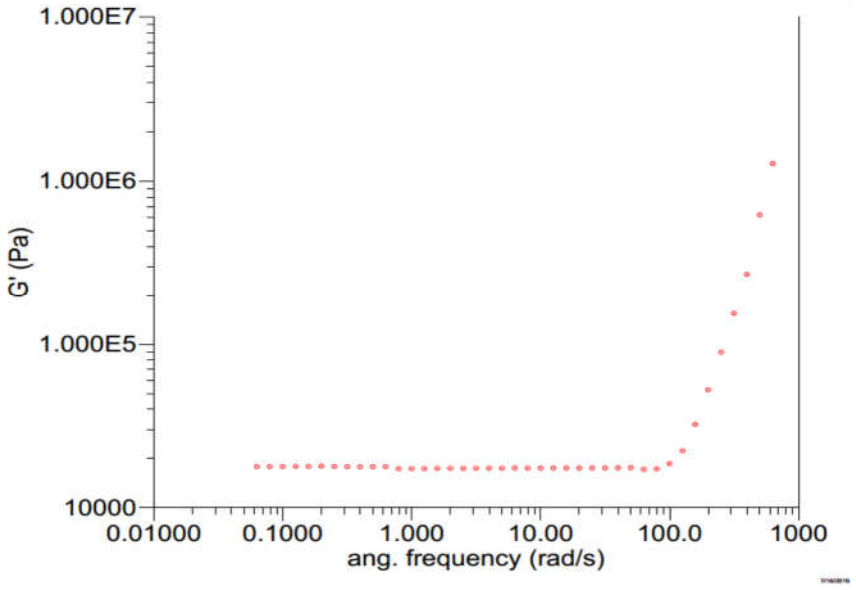

Figure 4: Frequency Sweep of an ADA-Gelatin hydrogel.

A frequency sweep (Figure 4) was done on the ADA-Gelatin to determine the appropriate parameters for the rheology experiments. The effects of frequency was tested over four orders of magnitude, from 0.06 rad/s to 630 rad/s. We did not observe the lower limit of the frequency-independent region, but the upper frequency limit was located; around 100 rad/s. In light of these

results, a testing frequency of 1 rad/s was chosen as it was in the middle of the frequency-independent linear region. A 1% strain was chosen for testing to provide a reasonable stress response as well as a small enough displacement that there was little risk of damaging the hydrogel.

Using the testing conditions of 1% strain applied at a rate of 1 rad/s, data was first taken with no light exposure to understand the behavior of the hydrogel under normal conditions. Graph A in Figure 5 shows the behavior of the hydrogel over a span of 10 minutes with no light exposure. The shear modulus does trend slightly upwards, indicating a slight stiffening effect from drying, but is a small change in the modulus overall. In graph B, a 15% gelatin hydrogel containing the normal 0.001% ADA was tested. The initial rise in the modulus is due to the superglue holding it to the plates curing. The modulus rise leveled out after 5 minutes and the UV light was turned on. From 5 to 10 minutes on the graph the UV light was on and the modulus was observed to drop. From 10 to 20 minutes, the sample was irradiated with white light which stopped the modulus from dropping anymore, but did not restore the modulus to its previously observed values. Finally, the UV light source was turned on again from 25 to 30 minutes, and the modulus can be seen to resume its downward trend. In graph C, a 10% gelatin hydrogel containing the normal 0.001% ADA was exposed to UV light continuously. The response in the modulus shows that there are diminishing returns experienced during extended periods of UV exposure, with a significant portion of the softening occurring in the first 5 minutes of UV exposure. It also appears that the modulus is approaching a minimum value over 30 minutes of UV exposure time. This makes sense as the ADA can only absorb UV light once and then it is in its *cis* isomer, which gives a firm limit on the amount of motion that each ADA molecule can contribute. Compounding this is the effects of attenuation of light in the hydrogel.

There is a maximum penetration depth that the UV light is able to achieve, and past that limit there will be no way to effect the change of the ADA from the *trans* to the *cis* isomer.

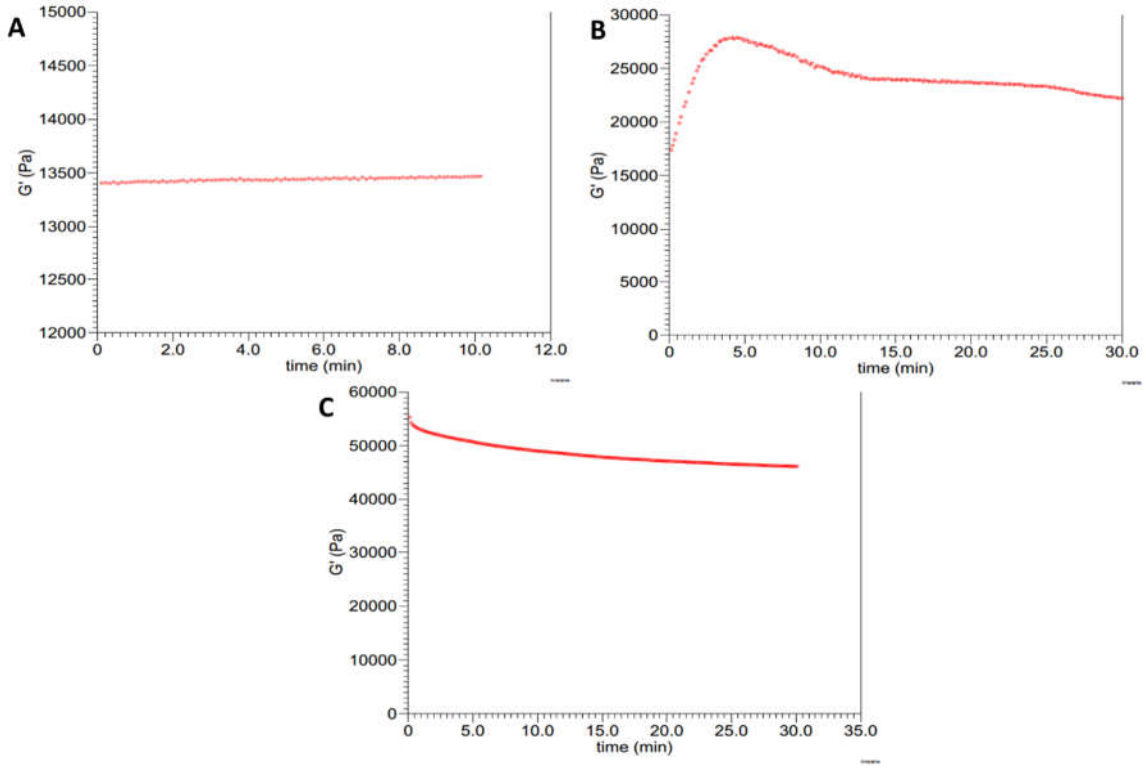

Figure 5: Rheological data. Plot A shows the behavior of a hydrogel under a no light condition for a baseline. Plot B shows an ADA-Gelatin hydrogel being glued to the platens and then being exposed to alternating UV and white light. Plot C shows an ADA-Gelatin hydrogel under constant UV exposure for 30 minutes.

To understand the bulk mechanical propertied of the hydrogels, the compressive modulus was measured (Figure 6). The modulus of the ADA-Gelatin hydrogels was first measured as synthesized. Then the same samples were irradiated with UV light for 5 minutes and retested to detect any changes upon exposure. Finally, the samples were exposed to white light for 5 minutes and retested to see if any changes observed after UV irradiation could be reversed. The control sample (10C), a 10% gelatin hydrogel with no ADA, showed no changes upon exposure to any of the lighting conditions, which indicates that the gelatin component does not interact

with the irradiating light in any way. The gelatin concentration was not expected to alter the nature of the hydrogel's interaction with UV light, so the control sample was run only at 10% gelatin and taken to be consistent across all concentrations of gelatin.

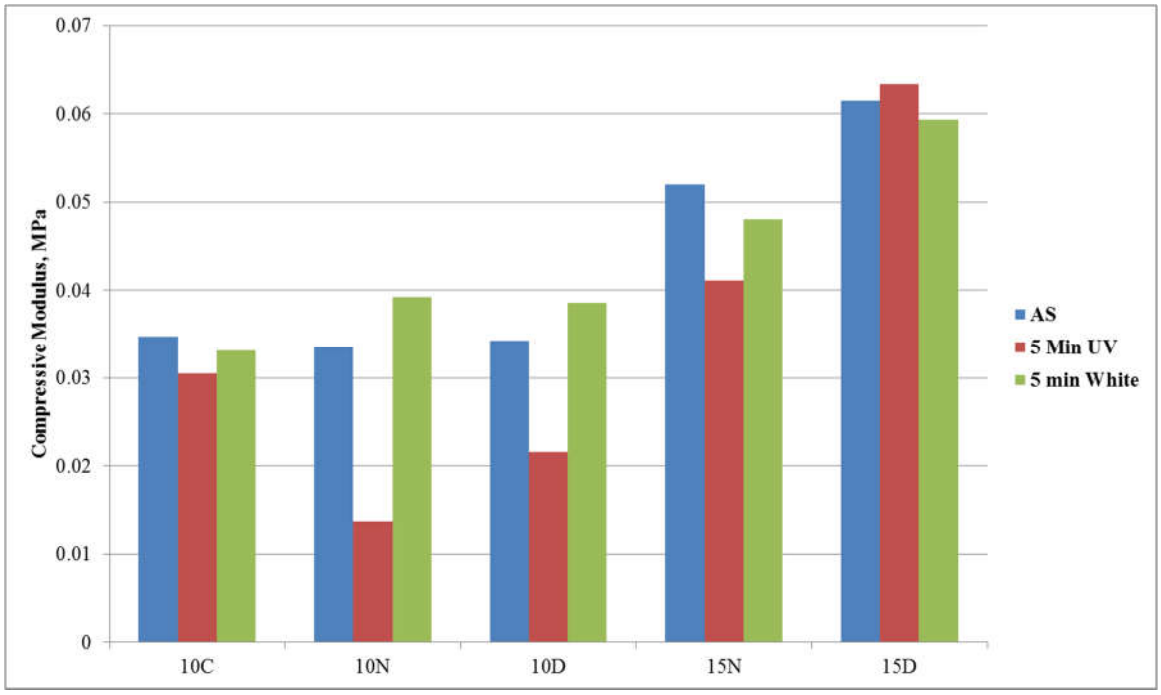

Figure 6: Data of Compressive moduli of ADA-Gelatin hydrogels.

The results of the tests of hydrogels consisting of 10% gelatin were summarized. The number on the x axis represents the gelatin concentration and the letter indicates the ADA concentration, with C representing control samples with no ADA, N representing samples with the normal 0.001% concentration of ADA, and D representing samples with the double concentration of 0.002% ADA. The 10% ADA-Gelatin hydrogels exhibited a reduction in modulus after exposure to UV light, down to roughly 40% of their pre-UV values. 10% gelatin hydrogels with a double amount of ADA exhibited a smaller reduction, and dropped to an average of 60% of their original modulus. In both cases, after exposure to white light the

modulus recovered, and the hydrogels were found to be roughly 15-20% stiffer than they were initially.

The samples with 15% gelatin did not exhibit as much response to the UV light as the 10% gelatin hydrogels. The 15% ADA-Gelatin hydrogels with a normal amount of ADA exhibited a reduction in modulus after exposure to UV light, down to roughly 80% of their pre-UV values. The 15% Gelatin hydrogels with a double amount of ADA did not show any response to the UV light. The modulus remained virtually unchanged across the UV and white light exposure conditions. White light restored the modulus to close to its original value for the normal ADA condition, but had virtually no effect on the double ADA hydrogels.

We would have expected that an increase in the amount of ADA would have increased the degree of stiffness loss upon exposure to UV light. This was not the case, however, with the hydrogels having a lower amount of ADA losing proportionately more stiffness upon exposure to UV light. It is likely that this is due to an increase in the attenuation of UV light as the ADA concentration is increased. The presence of ADA stops UV light so effectively that we were unable to use a photocrosslinking system, therefore we believe that the presence of additional ADA is reducing the maximum penetration depth of the UV light through absorption and reducing the magnitude of the effect of the UV light. This could also explain the lowered response from hydrogels containing larger concentrations of gelatin.

Another unexpected occurrence was that the modulus of the hydrogel was higher after it was exposed to white light than it was as synthesized for the 10% gelatin hydrogels. Virtually all of the ADA in the hydrogel should have already been in the *trans* isomer as the hydrogel was synthesized. One possibility is that the motion caused by the ADA contracting and expanding

may cause the hydrogel to retain some internal stress which manifests as a higher modulus. The confocal microscopy experiments indicated that the relaxation is not complete, so it is possible that some internal stress remains since the fluorescent beads did not return to their original positions. This may lead to fatigue damage if multiple cycles of UV and visible light are used to cause repeated contraction or relaxation.

CHAPTER 4

CONCLUSION & FUTURE DIRECTIONS

Thus far we know that the ADA-Gelatin Hydrogel is non-cytotoxic, and that its stiffness can be reduced by UV light and recovered by subsequent exposure to visible light. Additionally, we know that the macroscopic reduction in mechanical properties is accompanied by expansion and contraction on the microscale. This work focused on the mechanical changes that the hydrogels experienced, and showed that the shear modulus can be reduced with the application of UV light, but failed to show a reversibility with white light. Instead, the shear modulus slowed its rate of decline when exposed to white light rather than increasing its modulus to its previous value. We were able to manipulate the compressive modulus with UV light and we were also able to reverse the effects of the UV light with white light to restore the original modulus, at least for ADA-Gelatin hydrogels containing 10% gelatin. Finally, we were able to show motion on the cellular level using confocal microscopy and fluorescent beads. Preliminary tests have been done that show that this hydrogel is non-cytotoxic and that cells will proliferate when grown on it. These tests were done by another member of our lab (Brian O'Grady) and have shown that ADA-Gelatin hydrogels are compatible with a variety of cell types for extended periods of time, including MSCs and Fibroblasts for at least 3 weeks. This hydrogel platform shows some promise for use in tissue engineering as a phototunable scaffold material, but additional work must first be done to better understand the system before it can stand up to current options.

The first step is to characterize the network properties of the hydrogel more completely. The azobenzene derivative used in this work has a similar chemical structure as the mTG target, but it is significantly more sterically hindered. We currently do not know how effective crosslinking is for this molecule, and it is possible that the ADA is not integrating well into the gelatin network. Furthermore, it is possible that mTG is not able to create an isopeptide bond between the amine side chain of the ADA and a glutamine in the gelatin preventing cross linking. To ensure effective crosslinking, a peptide sequence could be added to our azobenzene derivative, using a method similar to that reported by Rosales *et al*.[34] Adding a peptide sequence would allow retention of the photoresponsive azobenzene, but add the specific moiety that the mTG enzyme is designed to target. Additionally, it would reduce steric hindrance by moving the site that binds to the enzyme further from the bulky azobenzene structure. Finally, it could increase the water solubility of the ADA. Currently, ADA is only slightly soluble in water, which necessitates its dissolution in ethanol. This limits its use in hydrogel-based systems since water solubility is key in such systems, and the use of ethanol as a solvent limits the amount of ADA that is safe to add when cells are present, since ethanol is cytotoxic.

A prime direction for future work would be to test lower concentrations of gelatin with the same ADA concentrations. This would answer whether or not the 15% gelatin hydrogels with ADA responded less to UV irradiation than similar hydrogels made with only 10% gelatin because of the increase in gelatin concentration or for some other reason. It would also make sense to study the attenuation caused by each formulation in order to understand the maximum penetration depth of the UV light and to see if the different gelatin concentrations influence the attenuation of the UV light.

Additionally, a calibration curve must be developed so that the change in the mechanical properties of the ADA-Gelatin can be precisely controlled using UV light. Additionally, since ADA also returns to the *trans* isomer thermodynamically, at both room temperature and physiological temperatures, the half-life of the *cis* isomer must also be determined since the ADA will relax over time and will need to be re-exposed to UV light to maintain constant mechanical properties. This is very important since our goal is to manipulate cells based on their response to the mechanical properties of the hydrogel, and if we cannot precisely control the mechanical properties of the hydrogels to hit specific modulus targets then it results in a significant reduction in the number of possible applications for this hydrogel.

Finally, the system should be tested for long term stability. From the confocal data, it was apparent that the gel does not move fully back to its original position after it is compressed with UV light. This could cause fatigue damage after multiple compression/relaxation cycles and would limit the applications for this system, especially if the system is discovered to thermally revert to the *trans* isomer fairly quickly after the UV exposure ends.

REFERENCES

[1]: Chan, B. P., and K. W. Leong. “Scaffolding in Tissue Engineering: General Approaches and Tissue-Specific Considerations.” European Spine Journal 17, no. Suppl 4 (December 2008): 467–79. doi:10.1007/s00586-008-0745-3.

[2]: Petersen, O. W., L. Rønnov-Jessen, A. R. Howlett, and M. J. Bissell. “Interaction with Basement Membrane Serves to Rapidly Distinguish Growth and Differentiation Pattern of Normal and Malignant Human Breast Epithelial Cells.” Proceedings of the National Academy of Sciences 89, no. 19 (October 1, 1992): 9064–68. doi:10.1073/pnas.89.19.9064.

[3]: Place, Elsie S., Nicholas D. Evans, and Molly M. Stevens. “Complexity in Biomaterials for Tissue Engineering.” Nature Materials 8, no. 6 (June 2009): 457–70. doi:10.1038/nmat2441.

[4]: Ott, Harald C., Thomas S. Matthiesen, Saik-Kia Goh, Lauren D. Black, Stefan M. Kren, Theoden I. Netoff, and Doris A. Taylor. “Perfusion-Decellularized Matrix: Using Nature’s Platform to Engineer a Bioartificial Heart.” Nature Medicine 14, no. 2 (February 2008): 213–21. doi:10.1038/nm1684.

[5]: Song, Jeremy J., and Harald C. Ott. “Organ Engineering Based on Decellularized Matrix Scaffolds.” Trends in Molecular Medicine 17, no. 8 (August 2011): 424–32. doi:10.1016/j.molmed.2011.03.005.

[6]: “Tissue-Engineered Bone Using Mesenchymal Stem Cells and a Bi... : Journal of Craniofacial Surgery.” LWW. Accessed July 12, 2016.

[7]: Chew, Sing Yian, Ruifa Mi, Ahmet Hoke, and Kam W. Leong. “The Effect of the Alignment of Electrospun Fibrous Scaffolds on Schwann Cell Maturation.” Biomaterials 29, no. 6 (February 2008): 653–61. doi:10.1016/j.biomaterials.2007.10.025.

[8]: Yim, Evelyn K. F., Ron M. Reano, Stella W. Pang, Albert F. Yee, Christopher S. Chen, and Kam W. Leong. “Nanopattern-Induced Changes in Morphology and Motility of Smooth Muscle Cells.” Biomaterials 26, no. 26 (September 2005): 5405–13. doi:10.1016/j.biomaterials.2005.01.058.

[9]: Jiang, Frank X., Bernard Yurke, Rene S. Schloss, Bonnie L. Firestein, and Noshir A. Langrana. “The Relationship between Fibroblast Growth and the Dynamic Stiffnesses of a DNA Crosslinked Hydrogel.” Biomaterials 31, no. 6 (February 2010): 1199–1212. doi:10.1016/j.biomaterials.2009.10.050.

[10]: Hollister, Scott J. “Porous Scaffold Design for Tissue Engineering.” Nature Materials 4, no. 7 (July 2005): 518–24. doi:10.1038/nmat1421.

[11]: Chuenjitkuntaworn, Boontharika, Wipawan Inrung, Damrong Damrongsri, Kongkwan Mekaapiruk, Pitt Supaphol, and Prasit Pavasant. “Polycaprolactone/hydroxyapatite Composite Scaffolds: Preparation, Characterization, and in Vitro and in Vivo Biological Responses of Human Primary Bone Cells.” Journal of Biomedical Materials Research Part A 94A, no. 1 (July 1, 2010): 241–51. doi:10.1002/jbm.a.32657.

[12]: Kim, Sinae, Sang-Soo Kim, Soo-Hong Lee, Seong Eun Ahn, So-Jung Gwak, Joon-Ho Song, Byung-Soo Kim, and Hyung-Min Chung. “In Vivo Bone Formation from Human Embryonic Stem Cell-Derived Osteogenic Cells in Poly(d,l-Lactic-Co-Glycolic Acid)/hydroxyapatite Composite Scaffolds.” Biomaterials 29, no. 8 (March 2008): 1043–53. doi:10.1016/j.biomaterials.2007.11.005.

[13]: Meinel, Lorenz, Vassilis Karageorgiou, Robert Fajardo, Brian Snyder, Vivek Shinde-Patil, Ludwig Zichner, David Kaplan, Robert Langer, and Gordana Vunjak-Novakovic. “Bone Tissue Engineering Using Human Mesenchymal Stem Cells: Effects of Scaffold Material and Medium

Flow." Annals of Biomedical Engineering 32, no. 1 (n.d.): 112–22. doi:10.1023/B:ABME.0000007796.48329.b4.

[14]: Da, Lawrence. "Transforming Growth Factor-Beta: A General Review." European Cytokine Network 7, no. 3 (1996 1996): 363–74.

[15]: Herbst, Roy S. "Review of Epidermal Growth Factor Receptor Biology." International Journal of Radiation Oncology*Biology*Physics 59, no. 2, Supplement (June 2004): S21–26. doi:10.1016/j.ijrobp.2003.11.041.

[16]: Chen, G., T. Ushida, and T. Tateishi. "Hybrid Biomaterials for Tissue Engineering: A Preparative Method for PLA or PLGA–Collagen Hybrid Sponges." Advanced Materials 12, no. 6 (March 1, 2000): 455–57. doi:10.1002/(SICI)1521-4095(200003)12:6<455::AID-ADMA455>3.0.CO;2-C.

[17]: Mooney, D. J., S. Park, P. M. Kaufmann, K. Sano, K. McNamara, J. P. Vacanti, and R. Langer. "Biodegradable Sponges for Hepatocyte Transplantation." Journal of Biomedical Materials Research 29, no. 8 (August 1, 1995): 959–65. doi:10.1002/jbm.820290807.

[18]: Schek, Rachel M., Erin N. Wilke, Scott J. Hollister, and Paul H. Krebsbach. "Combined Use of Designed Scaffolds and Adenoviral Gene Therapy for Skeletal Tissue Engineering." Biomaterials 27, no. 7 (March 2006): 1160–66. doi:10.1016/j.biomaterials.2005.07.029.

[19]: Larsen, Melinda, Vira V Artym, J Angelo Green, and Kenneth M Yamada. "The Matrix Reorganized: Extracellular Matrix Remodeling and Integrin Signaling." Current Opinion in Cell Biology, Cell-to-cell contact and extracellular matrix, 18, no. 5 (October 2006): 463–71. doi:10.1016/j.ceb.2006.08.009.

[20]: Lin, David C., Bernard Yurke, and Noshir A. Langrana. “Mechanical Properties of a Reversible, DNA-Crosslinked Polyacrylamide Hydrogel.” Journal of Biomechanical Engineering 126, no. 1 (March 9, 2004): 104–10. doi:10.1115/1.1645529.

[21]: Jiang, Frank X., Bernard Yurke, Rene S. Schloss, Bonnie L. Firestein, and Noshir A. Langrana. “The Relationship between Fibroblast Growth and the Dynamic Stiffnesses of a DNA Crosslinked Hydrogel.” Biomaterials 31, no. 6 (February 2010): 1199–1212. doi:10.1016/j.biomaterials.2009.10.050.

[22]: Gillette, Brian M., Jacob A. Jensen, Meixin Wang, Jason Tchao, and Samuel K. Sia. “Dynamic Hydrogels: Switching of 3D Microenvironments Using Two-Component Naturally Derived Extracellular Matrices.” Advanced Materials 22, no. 6 (February 9, 2010): 686–91. doi:10.1002/adma.200902265.

[23]: Kong, Na, Qing Peng, and Hongbin Li. “Rationally Designed Dynamic Protein Hydrogels with Reversibly Tunable Mechanical Properties.” Advanced Functional Materials 24, no. 46 (December 1, 2014): 7310–17. doi:10.1002/adfm.201402205.

[24]: Fancy, David A., and Thomas Kodadek. “Chemistry for the Analysis of Protein–protein Interactions: Rapid and Efficient Cross-Linking Triggered by Long Wavelength Light.” Proceedings of the National Academy of Sciences 96, no. 11 (May 25, 1999): 6020–24. doi:10.1073/pnas.96.11.6020.

[25]: Kloxin, April M., Andrea M. Kasko, Chelsea N. Salinas, and Kristi S. Anseth. “Photodegradable Hydrogels for Dynamic Tuning of Physical and Chemical Properties.” Science 324, no. 5923 (April 3, 2009): 59–63. doi:10.1126/science.1169494.

[26]: Yoshikawa, Hiroshi Y., Fernanda F. Rossetti, Stefan Kaufmann, Thomas Kaindl, Jeppe Madsen, Ulrike Engel, Andrew L. Lewis, Steven P. Armes, and Motomu Tanaka. “Quantitative

Evaluation of Mechanosensing of Cells on Dynamically Tunable Hydrogels." Journal of the American Chemical Society 133, no. 5 (February 9, 2011): 1367–74. doi:10.1021/ja1060615.

[27]: Guvendiren, Murat, and Jason A. Burdick. "Stiffening Hydrogels to Probe Short- and Long-Term Cellular Responses to Dynamic Mechanics." Nature Communications 3 (April 24, 2012): 792. doi:10.1038/ncomms1792.

[28]: Guan, Yue, Hai-Bo Zhao, Lei-Xiao Yu, Si-Chong Chen, and Yu-Zhong Wang. "Multi-Stimuli Sensitive Supramolecular Hydrogel Formed by Host–guest Interaction between PNIPAM-Azo and Cyclodextrin Dimers." RSC Advances 4, no. 10 (January 2, 2014): 4955–59. doi:10.1039/C3RA45461D.

[29]: Peng, Lu, Mingxu You, Quan Yuan, Cuichen Wu, Da Han, Yan Chen, Zhihua Zhong, Jiangeng Xue, and Weihong Tan. "Macroscopic Volume Change of Dynamic Hydrogels Induced by Reversible DNA Hybridization." Journal of the American Chemical Society 134, no. 29 (July 25, 2012): 12302–7. doi:10.1021/ja305109n.

[30]: Tamesue, Shingo, Yoshinori Takashima, Hiroyasu Yamaguchi, Seiji Shinkai, and Akira Harada. "Photoswitchable Supramolecular Hydrogels Formed by Cyclodextrins and Azobenzene Polymers." Angewandte Chemie International Edition 49, no. 41 (October 4, 2010): 7461–64. doi:10.1002/anie.201003567.

[31]: Zhao, Yan-Li, and J. Fraser Stoddart. "Azobenzene-Based Light-Responsive Hydrogel System." Langmuir 25, no. 15 (August 4, 2009): 8442–46. doi:10.1021/la804316u.

[32]: Hartley, G. S. "The Cis-Form of Azobenzene." Nature 140 (August 1, 1937): 281. doi:10.1038/140281a0.

[33]: Ikeda, Tomiki, and Osamu Tsutsumi. "Optical Switching and Image Storage by Means of Azobenzene Liquid-Crystal Films." Science 268, no. 5219 (June 30, 1995): 1873.

[34]: Jog, Parag V., and Mary S. Gin. “A Light-Gated Synthetic Ion Channel.” Organic Letters 10, no. 17 (September 1, 2008): 3693–96. doi:10.1021/ol8013045.

[35]: Liu, Z. F., K. Hashimoto, and A. Fujishima. “Photoelectrochemical Information Storage Using an Azobenzene Derivative.” Nature 347, no. 6294 (October 18, 1990): 658–60. doi:10.1038/347658a0.

[36]: Yesodha, Sandhya K., Chennakattu K. Sadashiva Pillai, and Naoto Tsutsumi. “Stable Polymeric Materials for Nonlinear Optics: A Review Based on Azobenzene Systems.” Progress in Polymer Science 29, no. 1 (January 2004): 45–74. doi:10.1016/j.progpolymsci.2003.07.002.

[37]: Beharry, Andrew A., and G. Andrew Woolley. “Azobenzene Photoswitches for Biomolecules.” Chemical Society Reviews 40, no. 8 (July 14, 2011): 4422–37. doi:10.1039/C1CS15023E.

[38]: Rosales, Adrianne M., Kelly M. Mabry, Eric Michael Nehls, and Kristi S. Anseth. “Photoresponsive Elastic Properties of Azobenzene-Containing Poly(ethylene-Glycol)-Based Hydrogels.” Biomacromolecules 16, no. 3 (March 9, 2015): 798–806. doi:10.1021/bm501710e.

[39]: Banghart, Matthew, Katharine Borges, Ehud Isacoff, Dirk Trauner, and Richard H. Kramer. “Light-Activated Ion Channels for Remote Control of Neuronal Firing.” Nature Neuroscience 7, no. 12 (December 2004): 1381–86. doi:10.1038/nn1356.

[40]: Yuan, Quan, Yunfei Zhang, Tao Chen, Danqing Lu, Zilong Zhao, Xiaobing Zhang, Zhenxing Li, Chun-Hua Yan, and Weihong Tan. “Photon-Manipulated Drug Release from a Mesoporous Nanocontainer Controlled by Azobenzene-Modified Nucleic Acid.” ACS Nano 6, no. 7 (July 24, 2012): 6337–44. doi:10.1021/nn3018365.

[41]: Schindelin, Johannes, Ignacio Arganda-Carreras, Erwin Frise, Verena Kaynig, Mark Longair, Tobias Pietzsch, Stephan Preibisch, et al. “Fiji: An Open-Source Platform for

Biological-Image Analysis." Nature Methods 9, no. 7 (July 2012): 676–82. doi:10.1038/nmeth.2019.